

Languages Transferred Within the Encoder: On Representation Transfer in Zero-Shot Multilingual Translation

Zhi Qu[†] Chenchen Ding^{†‡} Taro Watanabe[†]

[†]Nara Institute of Science and Technology, Japan
{qu.zhi.pv5, taro}@is.naist.jp

[‡]National Institute of Information and Communications Technology, Japan
chenchen.ding@nict.go.jp

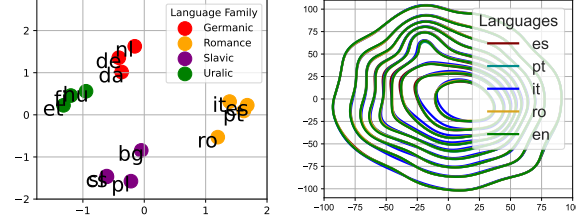
Abstract

Understanding representation transfer in multilingual neural machine translation can reveal the representational issue causing the zero-shot translation deficiency. In this work, we introduce the identity pair, a sentence translated into itself, to address the lack of the base measure in multilingual investigations, as the identity pair represents the optimal state of representation among any language transfers. In our analysis, we demonstrate that the encoder transfers the source language to the representational subspace of the target language instead of the language-agnostic state. Thus, the zero-shot translation deficiency arises because representations are entangled with other languages and are not transferred effectively to the target language. Based on our findings, we propose two methods: 1) low-rank language-specific embedding at the encoder, and 2) language-specific contrastive learning of the representation at the decoder. The experimental results on Europarl-15, TED-19, and OPUS-100 datasets show that our methods substantially enhance the performance of zero-shot translations by improving language transfer capacity, thereby providing practical evidence to support our conclusions.¹

1 Introduction

State-of-the-art neural machine translation systems are adaptable to multilingualism, resulting in a single encoder-decoder model that executes arbitrary translations by adding a tag specified to the target language at the beginning of source sentence (Firat et al., 2016; Johnson et al., 2017; Wu et al., 2021). Multilingual neural machine translation (MNMT) is theoretically attractive because zero-shot translations, i.e., translations unseen in training, allow the training of a multilingual model with minimal cost. Unfortunately, the performance of zero-shot translations always lags behind (Aharoni et al., 2019;

¹Partial works done during Zhi Qu’s internship at ASTREC of NICT, Japan. Our codes are available at <https://github.com/zhiqu22/ZeroTrans>.



(a) Cluster by target languages (b) Semantic alignments

Figure 1: Different analytical methods lead to different conclusions. 1a means the target language family clusters the representations of translations from English (en) to other languages through the encoder. 1b indicates the encoder semantically aligns different source languages. Language codes in this work follow ISO 639-1, and Appendix D provides details of those figures.

Arivazhagan et al., 2019a; Gu et al., 2019; Yang et al., 2021; Pan et al., 2021; Chen et al., 2023).

Representational analysis in MNMT models guides the improvement of zero-shot translation. However, two different perspectives are demonstrated by prior works: 1) the encoder clusters the different translation representations by the target language (Kudugunta et al., 2019; Liu et al., 2021), as shown in Figure 1a; 2) an ideal encoder is considered to learn only language-agnostic representations, where general cross-lingual features are modeled and transferred among languages (Pan et al., 2021; Gu and Feng, 2022; Gao et al., 2023), as shown in Figure 1b. In this work, our investigation proves that these two perspectives are two sides of the same coin, as the encoder aligns translation representations from different source languages within the subspace of the target language.

We introduce the identity pair, which is a pseudo pair translating a sentence to itself, as a proxy for the optimal representation of a language. We then use multiple analytical methods, including singular value canonical correlation analysis (SVCCA) (Raghu et al., 2017) and t-distributed stochastic neighbor embedding (t-SNE) (van der Maaten and Hinton, 2008), to systematically analyze and quantify the representation transfer in MNMT models.

We show that transferring representations from the source language to the target language is a major task of the encoder and is entirely accomplished by the encoder. Therefore, the zero-shot translation deficiency arises from the translation representations being entangled with other languages rather than being effectively transferred to the expected target language within the encoder.

Guided by our findings, we propose two methods for the encoder and decoder, respectively, to improve multilingual representations: **Low-Rank Language-specific Embedding (LOLE)** is applied to bias the representations in the subspaces of target languages at the encoder; and **Language-specific Contrastive Learning of Representations (LCLR)** is applied at the decoder to isolate representational space across languages. We evaluated the proposed methods on three benchmarks, Europarl-15 (Koehn et al., 2005), TED-19 (Ye et al., 2018), and OPUS-100 (Zhang et al., 2020a; Yang et al., 2021), for two automatic metrics, SacreBLEU (Post, 2018) and BERTScore (Zhang et al., 2020b). The experimental results show that our methods outperform strong baselines in training from scratch because of improved representational transferability. Our methods also perform effectively in fine-tuning, even though pre-trained models are trained by different strategies of language tags, which proves that target language information on the encoder side consistently benefits MNMT.

2 Background

2.1 Multilingual Neural Machine Translation

Johnson et al. (2017); Wu et al. (2021) demonstrated that the training strategy of adding a language tag at the beginning of the input sentence on the encoder side boosts the zero-shot translation capacity of the MNMT model. Given a multilingual corpus \mathbb{C} that covers a set of t languages, a set of their corresponding language tags exists: $\mathbb{L} = \{l_1, l_2, \dots, l_t\}$. For a source-target sentence pair (\mathbf{x}, \mathbf{y}) , i.e., $\mathbf{x} = x_1, x_2, \dots, x_n$ and $\mathbf{y} = y_1, y_2, \dots, y_m$, the training data consists of a pair in form of $(\mathbf{x}, l, \mathbf{y})$, where l is the language tag of \mathbf{y} that instructs translation from \mathbf{x} into language l . The model is trained over all pairs in \mathbb{C} to optimize the following cross-entropy loss:

$$\mathcal{L}_{ce} = - \sum_{\mathbf{x}, l, \mathbf{y} \in \mathbb{C}} \log p(\mathbf{y}|l, \mathbf{x}; \theta), \quad (1)$$

where $p(\mathbf{y}|l, \mathbf{x}; \theta)$ is the probability distribution of \mathbf{y} and θ represents the model parameters.

2.2 Prior Investigations of MNMT

Two tools are used in prior investigations: 1) The t-distributed stochastic neighbor embedding (t-SNE) (van der Maaten and Hinton, 2008) converts similarities between a set of vector representations to joint probabilities; 2) The singular value canonical correlation analysis (SVCCA) (Raghu et al., 2017) compares the similarity between two vector representations². The visualization using t-SNE shows that translation representations, which belong to different source languages but with the same semantics, are aligned at the output of the encoder (Pan et al., 2021; Gao et al., 2023), suggesting the ideal encoder is language-agnostic. Specifically, translation representations from different source languages are transferred to a language-agnostic state before being transferred to the target language. On the contrary, the investigation of Kudugunta et al. (2019) based on SVCCA demonstrates that translation representations possess the features of the target language. However, the results derived from measuring SVCCA scores between real translation pairs are disturbed by the lack of base measures. For instance, the translation from English to German, denoted by $\text{en} \rightarrow \text{de}$, cannot serve as a base measure for the translation from another language $\mathbf{x} \rightarrow \text{de}$, because the representation of $\text{en} \rightarrow \text{de}$ is not equivalent to the representation of de .

3 Investigating Representation Transfer in MNMT

We conduct preliminary experiments to investigate representations by introducing identity pairs as base measures. Two different datasets, Europarl-15 (Koehn et al., 2005; Dabre and Kurohashi, 2019) and TED-19 (Ye et al., 2018), are applied to verify whether our observations are general. Appendix B introduces the detailed information of those two datasets. Then, following Kudugunta et al. (2019), our investigation is based on Transformer models with 6 encoder and decoder layers, where Appendix C introduces the detailed model settings.

3.1 Identity Pairs

Identity pairs refer to the translation pairs translating from themselves into themselves to present the optimal state of processing language features, i.e., the semantics and syntax of the source sen-

²We follow Liu et al. (2021) to measure SVCCA scores at the sentence level. Appendix A shows how to compute SVCCA scores.

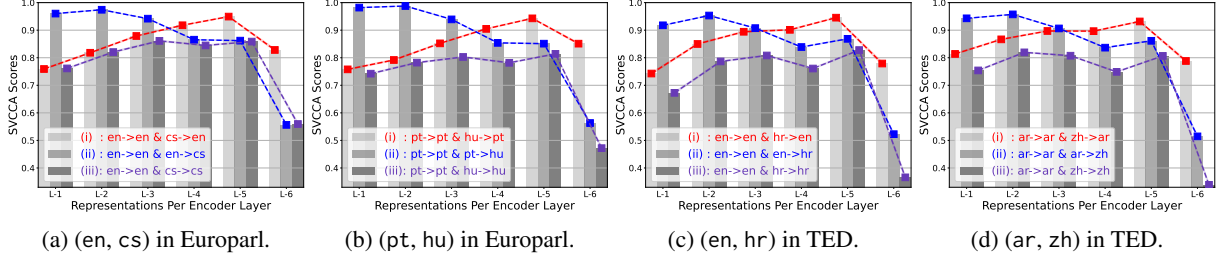


Figure 2: Visualizations of layer-wise SVCCA scores for the encoder. (①, ②) indicate the source language and target language, respectively. The analyzed models have 6 encoder layers, and the analysis based on models with 8 and 10 encoder layers shows the same tendency, which is shown in Appendix E.

tence by the model. On the encoder side, we derive the representation from a language translating to itself, i.e., (x, l', x) , where l' is the language tag of x , with the aim of recovering the source sentence from the hidden representations without inference on the decoder side. We derive the representation in the decoder from the gold translation of (x, l', x) .

We use SacreBLEU (Papineni et al., 2002; Post, 2018) to evaluate the translation quality of 6 identity pairs, which are generated by inference. The scores of $en \rightarrow en$, $de \rightarrow de$, and $pt \rightarrow pt$ in Europarl-15 are 73.49, 61.04, and 71.97, which significantly outperform 44.04 of $de \rightarrow en$, 36.63 of $en \rightarrow de$, and 46.24 of $en \rightarrow pt$, respectively. Similarly, $en \rightarrow en$, $tr \rightarrow tr$, and $vi \rightarrow vi$ in TED-19 obtain scores of 72.52, 36.58 and 59.26, which are higher than 34.92 of $de \rightarrow en$, 14.81 of $en \rightarrow tr$, and 29.78 of $en \rightarrow vi$, respectively. Such high scores in the identity pair are caused by that short sentences are recovered from hidden representations perfectly, and long sentences only have a few changes in word selection. Such evidence suggests that identity pairs can serve as base measures for comparing representations because the identity pair is a proxy for the optimal representation of a language, specifically, $x \rightarrow en$ are expected to be close to $en \rightarrow en$ in the representational space.

3.2 Language Transfer Within the Encoder

Given two languages ① and ②, two sentences x of ① and y of ② are grouped by three cases when comparing the representations of the encoder: (i) comparing $(x, l^①, x)$ and $(y, l^①, x)$ to show how target language features are encoded³; (ii) comparing $(x, l^①, x)$ and $(x, l^②, y)$ to show how source language features are encoded; (iii) comparing two different identities, $(x, l^①, x)$ and $(y, l^②, y)$.

The two models trained by Europarl-15 and

³ $(x, l^①, x)$ indicates the identity of ①, i.e., ① \rightarrow ①, and $(y, l^①, x)$ indicates a sentence of ② translating to the sentence of ① instructed by the language tag of ①, i.e., ② \rightarrow ①.

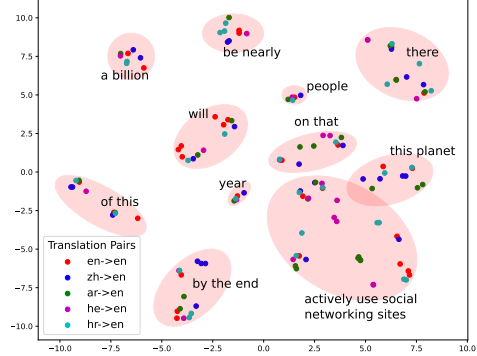


Figure 3: t-SNE plot of the token-level alignment between $en \rightarrow en$ and $x \rightarrow en$ in TED-19. Each point is a token’s representation collected from the output of the encoder. Representations of different tokens are clustered by the semantics, which are denoted by English phrases, where the overall variance is 0.09. Appendix H shows the more details.

TED-19 show the same tendency in Figure 2, that is, the language features for ① of (i) consistently increase in both cases involving the central language in Figures 2a and 2c, and non-central languages in Figures 2b and 2d. The target language feature of ① emerges as the primary factor that affects representations at the fifth and sixth layers when the cases of (i), (ii), and (iii) are compared. Therefore, we can conclude that the language features of the representations are transferred to the target side within the encoder. Meanwhile, we also observe that the scores of (iii) are close to or even exceed those of (ii) at some layers both in Figure 2. This proves that the feature of the source language is not the primary factor for representations in the encoder because representations are transferred to the subspaces of target languages. Thus, the comparison between (ii) and (iii) supports the conclusion that language transfer is completed within the encoder.

On the other side, identity pairs also allow the measurement of the alignment of different languages in the target language space through t-SNE. Compared with the sentence-level measurement of Pan et al. (2021); Gao et al. (2023), we measure the alignment of representations at the token level. As

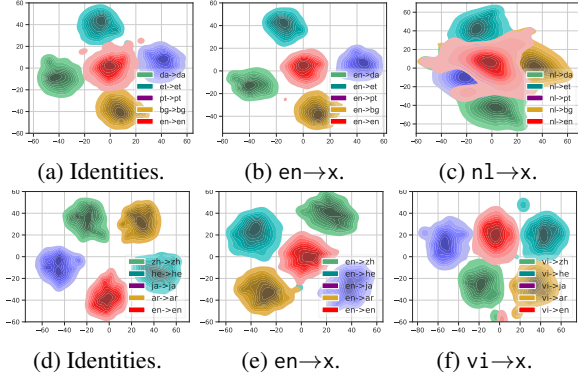


Figure 4: Visualizations for the encoder’s output by t-SNE and BiKDE. 4a, 4b and 4c are measured in Europarl-15. 4d, 4e and 4f are measured in TED-19.

shown in Figure 3, semantic similarity causes the representations to cluster together. Moreover, as shown in Appendix H, these representations are not clustered before being processed by the encoder, and the case with different target languages has a higher overall variance. Combined with the finding that the encoder transfers the representation of the source language to the target language, the evidence further suggests that there is no general and cross-lingual state for directly sharing semantic information within the encoder, and the alignment shown in Figure 1b occurs in the representational subspace of the target language.

3.3 Entanglements Hindering the Transfer

Although the investigation in Section 3.2 shows that the representations gradually transfer to the target language in a translation pair, the representation spaces of multiple languages may potentially entangle with each other, resulting in the failure of the zero-shot translation (Qu and Watanabe, 2022). To further illustrate the relationship between different languages, we use t-SNE and BiKDE to visualize the representations at the output of the encoder for the several identity pairs in Europarl-15 and TED-19. Figures 4a and 4d show that different identity pairs are uniformly distributed in the representational space. This distribution proves again that the encoder is language-specific because each language has an isolated representational subspace.

Compared with identity pairs that represent the ideal capability of the model in processing languages, the distributions plotted in Figures 4b and 4e reflect the actual capacity for the supervised translation of $en \rightarrow x$. Figures 4b and 4e show the distribution of representations in the pairs translating from en, which are similar to that of identity pairs. The difference between identity pairs

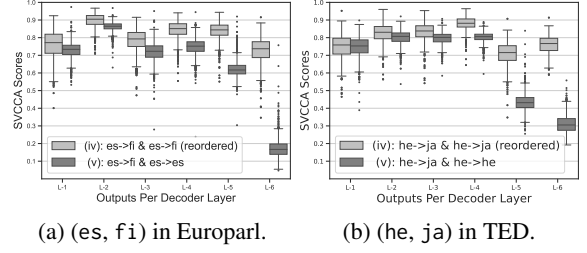


Figure 5: Visualizations of layer-wise SVCCA scores for the decoder. (3, 4) shows the involved languages.

and supervised language pairs can be attributed to the influence of the source language information, which hinders the full use of the target language information learned by the encoder.

Moreover, the language-specific subspaces cannot be clearly separated for zero-shot translations, as shown in Figures 4c and 4f. Specifically, all representations are entangled around the supervised language pair of $x \rightarrow en$, which hinders these representations from transferring into the ideal subspaces of the target language. This aligns with Qu and Watanabe (2022) that non-central languages are entangled with the central language, i.e., English, which explains the weakness of zero-shot translation compared with supervised translation, namely, the focal point for improving the transferability of representations is to improve the extent of language transfer in the encoder.

3.4 Language Features in the Decoder

The decoder works on representations with target language features because the source language has already been transferred into the target language subspace (Section 3.2). Therefore, representational entanglements (Section 3.3) also affect the decoder. We further investigate the importance of target language features versus semantics in the decoder. Given two sentences x of language ③ and y of language ④, the decoder representation of $(x, l^{\text{④}}, y)$ is considered as the base measure. We group two cases: (iv) For each sentence in a test set, we identify the pair $(x', l^{\text{④}}, y')$ with the lowest SVCCA score in the encoder representation to derive a x' that is distant from x . Then, we compare it with the base measure to show the importance of target language features; (v) We compare the base measure and $(y, l^{\text{④}}, y)$ to show the importance of semantics. The two scenarios shown in Figure 5 present the same trend, which is that (iv) maintains high scores despite their semantics being entirely different. At the top layers of the decoder, the gradually increasing difference between (iv) and (v) confirms that the decoder tends to learn the target

language specificity (Sen et al., 2019). However, Figure 5 shows that, for (iv), a wider interquartile range exists at the bottom layers of the decoder, and its scores are close to those of (v), which implies the weakness of the distinguishing languages in zero-shot translations.

4 Encouraging Representation Transfer

To validate the findings in Section 3, we propose two methods on the encoder and decoder sides, respectively, to improve transferability. Based on the findings in Sections 3.2 and 3.3, improving the extent of language transfer in the encoder can overcome the hindered representations of zero-shot language pairs. We introduce a learnable embedding referred to as Low-rank Language-specific Embedding (LOLE). It serves as biases to force representations to transfer into the target language with negligible cost. Based on the findings in Section 3.4, the capacity for multilingual features is insufficient at the lower layers of the decoder. We introduce Language-specific Contrastive Learning of Representations (LCLR) as an training extra task to regularize the representations to specify the representational boundary for each language.

4.1 Low-Rank Embedding for the Encoder

Let $\mathbb{E} = \{e^1, e^2, \dots, e^p\}$, $e^j \in \mathbb{R}^d$, be a set of embeddings that correspond one-to-one with the languages in \mathbb{L} . For a translation (x, l, y) , the embedding in \mathbb{E} corresponding to l is denoted by e^l . The hidden representation $\mathbf{H}^z = \{h_1^z, h_2^z, \dots, h_q^z\}$, where $\mathbf{H}^z \in \mathbb{R}^{q \times d}$, is extracted before the feed-forward network (FFN) (Khandelwal et al., 2021; Xu et al., 2023; Deguchi et al., 2023) at the z -th encoder layer. Then, we broadcast e^l to \mathbf{E}^l , $\mathbf{E}^l \in \mathbb{R}^{q \times d}$, and we bias \mathbf{H}^z to $\hat{\mathbf{H}}^z$:

$$\hat{h}_i^z = h_i^z + e_i^l, \quad (2)$$

where $\hat{\mathbf{H}}^z$ is the input for the FFN of the z -th encoder layer (Figure 6a). We execute this biasing at the second-top encoder layer to ensure sufficient capacity for fusing representations and language information, while implicitly allowing lower layers to focus on surface-level information.

The simple language categorization by embedding may lead to a risk of dimensional collapse in the latent space (Jing et al., 2022). Thus, we reduce the dimension of \mathbb{E} to d^e to allow biasing in a low rank, and add it to the head of h_i^z to simultaneously encourage language transfer and minimize the influence on representations (Hu et al.,

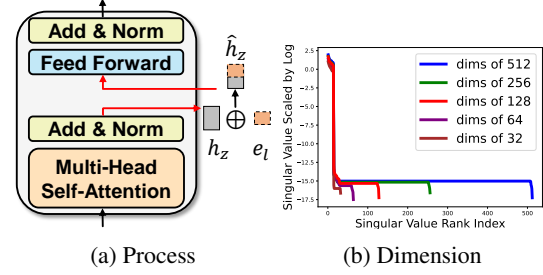


Figure 6: Illustrations of LoLE. 6a shows the process in an encoder layer, where \oplus represents the operation of Equation(2) at a low rank. 6b is the spectrum with different dimensions of \mathbb{E} , which illustrates the singular values of the covariance matrix of \mathbb{E} in sorted order and logarithmic scale.

2021). Figure 6b is a spectrum used to illustrate dimensional collapse using a comparison of different d^e in Europarl-15. The spectrum shows that larger dimensions are primarily composed of noise, whereas a dimension that is too small adversely affects the learning of key features.

4.2 Contrastive Learning for the Decoder

Given a training batch, we extract hidden representations from the output of each decoder layer and apply averaged pooling to obtain a fixed-dimensional representation for each sentence. To avoid dimensional collapse (Tian, 2022; Jing et al., 2022), we also use the head of the representation for contrastive learning, i.e., the vectors in the batch $\mathbb{B} = \{\bar{h}_1, \bar{h}_2, \dots\}$, $\bar{h}_i \in \mathbb{R}^{d^h}$, $d^h < d$.

To prevent a potential invalid training objective in sampling caused by the skewed distribution in a batch, we first define $\mathbb{B}' \subseteq \mathbb{B}$ by omitting instances that do not share their target language with any other instance in \mathbb{B} . For a given instance of $h^{anc} \in \mathbb{B}'$, which is the anchor in contrastive learning, we let \mathbb{B}^+ denote the subset of \mathbb{B}' , including instances with the same target language as h^{anc} , where $|\mathbb{B}^+| > 1$. Likewise, we define a subset for negative instance $\mathbb{B}^- = \mathbb{B}' \setminus \mathbb{B}^+$. For contrastive learning, we randomly sample the positive instance h^{pos} from \mathbb{B}^+ and sample k negative instances h^{neg} from \mathbb{B}^- . Additionally, if $k > |\mathbb{B}^-|$, we dynamically clip k to $|\mathbb{B}^-|$. Formally, the objective of LCLR is formulated as

$$\begin{aligned} \mathcal{L}_{ctr} = & - \sum_{h^{anc} \in \mathbb{B}'} \log \frac{e^{s^+}}{e^{s^+} + \sum_{i=1}^k e^{s_i^-}}, \\ s^+ = & \text{sim}(h^{anc}, h^{pos}), h^{pos} \in \mathbb{B}^+, \\ s_i^- = & \text{sim}(h^{anc}, h_i^{neg}), h_i^{neg} \in \mathbb{B}^-, \end{aligned} \quad (3)$$

where $\text{sim}(\cdot)$ calculates the similarity of representations using the cosine similarity. The final training

objective is the sum of Equations 1 and 2, i.e.,

$$\mathcal{L} = \mathcal{L}_{ce} + \mathcal{L}_{ctr}. \quad (4)$$

5 Experiments

5.1 Setup

Datasets Our experiments comprise three English-centric scenarios, i.e., the training and validation sets only involving translation pairs translating to en or from en. 1) Europarl-15 is a sub-collection of MMCR4NLP (Koehn et al., 2005; Dabre and Kurohashi, 2019), resulting in 5.3 million training translation pairs. 2) TED-19 collects 19 languages from TED Talks (Ye et al., 2018), where the training set comprises 6.5 million pairs in total. 3) OPUS-100 (Zhang et al., 2020a; Yang et al., 2021) consists of 95 languages and 109.2 million training pairs. Generally, the validation and test sets of a pair contain 2,000 pairs. More detailed information of those datasets can be found in Appendix B.

Models In experiments of training from scratch, we implement a Transformer model with 6 encoder and decoder layers. Then, three pre-trained models⁴ are utilized in our experiments of fine-tuning, including M2M-418M, M2M-1.2B (Fan et al., 2020) and mBART50 (Liu et al., 2020). Based on the ablation study conducted in the validation set in Europarl-15 and TED-19 shown in Appendix F, we apply LOLE in the fifth encoder layer, set d^e to 128, and set d^h and k of LCLR to 64 and 30, respectively. We enlarge d^e to 256 and d^h to 128 for models trained on OPUS-100 and three pre-trained models because they involve more languages. When we solely apply LCLR, we set the position to the bottom decoder layer based on the findings in Section 3.4. When we integrate both LOLE and LCLR into a model, we relocate LCLR to the second-bottom decoder layer because of the improved language features of the encoder representations. More detailed settings of models and training details can be found in Appendix C.

Baselines and Evaluation The vanilla Transformer (Vaswani et al., 2017; Johnson et al., 2017) is a baseline in experiments, denoted by VANILLA. Additionally, three representative methods are reproduced in experiments of training from scratch with our datasets and settings: 1) SEMALI (Pan

et al., 2021), which is a state-of-the-art MNMT model without fine-tuning that uses contrastive learning in the encoder output for semantic alignment; 2) DISPOS (Liu et al., 2021), which removes one residual connection in the encoder to weaken the source language information; and 3) TLP (Yang et al., 2021), which has an extra loss introduced to identify the language of the decoder’s output representation. In the evaluation, we set the beam size to 4 in inference. We not only use SacreBLEU (Papineni et al., 2002; Post, 2018) to evaluate the quality of inferences but also report BERTScore (Zhang et al., 2020b) of inferences at the representation level. We also conduct statistical significance testing (Koehn, 2004) using paired bootstrap resampling with 1,000 iterations and 0.5 resampling ratio, consequently, the case of $p < 0.05$ means that the difference is significant.

5.2 Results

Table 1 shows the experimental results of training from scratch. Our proposed methods always perform best in comparison with strong baselines, or are close to the best method. In supervised translations of three benchmarks of Europarl-15/TED-19/OPUS-100, LOLE shows divergent results of 0.13/-0.04/-0.22 on en→x and 0.11/0.05/-0.02 on x→en. Similarly, LCLR shows diverse results of -0.05/-0.01/-0.03 and 0.04/-0.01/0.07, respectively. Then, BOTH achieves the results of 0.18/-0.02/0.03 on en→x and 0.12/0.12/-0.03 on x→en. The results suggest that our model is comparable to VANILLA on supervised translations. Therefore, given that the improvement of zero-shot translation potentially reduces the quality of supervised translations (Gu et al., 2019; Zhang et al., 2020a; Liu et al., 2021), our methods are stronger in avoiding the degeneration of supervised language pairs compared with other methods. In zero-shot translations, BOTH outperforms VANILLA 1.55/1.33/2.93 for BLEU and 0.58/1.02/3.12 for BERTScore. In an assessment of the qualities individually, LOLE achieves gains of 1.53/1.22/2.85 for BLEU and 0.54/0.91/3.34 for BERTScore, and LCLR improves 1.06/0.14/0.09 scores for BLEU and 0.39/0.13/0.06 scores for BERTScore. The results indicate that our proposed methods are orthogonal. Moreover, the significant testing shows that our methods substantially improve the zero-shot translation capacity in training from scratch.

Table 2 shows the experimental results of fine-tuning. For M2M-418M, compared with F.T., our

⁴Notably, those models are trained by adding a source language tag at the encoder and a target language tag at the decoder. In fine-tuning, we keep their strategy, because it is not conflict with adding extra target information by LOLE.

Method	Europarl-15						TED-19						OPUS-100					
	BLEU			B.S.			BLEU			B.S.			BLEU			B.S.		
	en→	→en	zero.	en→	→en	zero.	en→	→en	zero.	en→	→en	zero.	en→	→en	zero.	en→	→en	zero.
VANILLA	37.49	43.39	24.65	88.50	95.71	84.27	24.53	29.67	11.98	83.77	93.54	77.74	23.37	28.30	5.04	69.98		
DisPos	37.15	43.37	25.89	88.39	95.72	84.69	24.08	29.43	12.80	83.62	93.49	78.36	22.72	28.24	5.58	70.74		
TLP	37.41	43.28	24.96	88.47	95.71	84.40	24.44	29.62	12.74	83.73	93.53	78.24	23.41	28.30	4.60	69.40		
SEMALI	37.27	43.06	25.25	88.42	95.69	84.43	23.55	28.67	13.45	83.43	93.36	78.91	22.35	28.29	6.42	72.00		
LOLE	37.62	43.50	26.09	88.51	95.72	84.81	24.39	29.72	13.20	83.74	93.54	78.65	23.15	28.28	7.92 [†]	73.32[†]		
LCLR	37.44	43.43	25.71	88.46	95.72	84.66	24.46	29.66	12.12	83.76	93.54	77.87	23.34	28.37	5.11	70.04		
BOTH	37.67[†]	43.51	26.20[†]	88.50	95.72	84.85[†]	24.49	29.79	13.31	83.76	93.56	78.76	23.40	28.27	7.97[†]	73.10 [†]		

Table 1: Averaged scores for experiments of training from scratch. BOTH in the table means using LOLE and LCLR together; en→ and →en abbreviates en→x and x→en; zero. means zero-shot language pairs; and B.S. abbreviates BERTScore. We only report zero-shot language pairs of OPUS-100 because BERTScore does not support some pairs in supervised translations, but zero-shot translation pairs of OPUS-100 are involved only with 6 languages, which are supported. The bold numbers indicate the best results and the numbers with † are significantly better than baselines according to the significance test with $p < 0.05$.

Method	BLEU			BERTScore		
	en→	→en	zero.*	en→	→en	zero*
M2M-418M	21.88	26.43	14.51	82.52	93.25	79.26
F.T.	26.68	32.95	17.46	84.47	94.30	80.79
LOLE	26.81	33.16	17.52	84.51	94.31	80.84
LCLR	26.81	33.67[†]	17.65	84.47	94.40	80.88
BOTH	26.83[†]	33.63 [†]	17.68[†]	84.49	94.38	80.90[†]
M2M-1.2B	24.32	28.94	15.95	83.17	93.72	79.75
F.T.	27.71	34.97	18.48	84.71	94.53	81.14
LOLE	28.29 [†]	34.12	18.67 [†]	84.91 [†]	94.48	81.26[†]
LCLR	28.26 [†]	34.54	18.64	84.90 [†]	94.50	81.22
BOTH	28.37[†]	34.59	18.69[†]	84.92[†]	94.51	81.23
mBART50	25.28	33.50	6.92	83.93	94.43	72.91
F.T.	27.17	33.96	5.58	84.64	94.36	72.96
LOLE	27.19	33.93	7.28	84.60	94.37	73.86
LCLR	27.07	34.02	9.69[†]	84.59	94.38	75.31 [†]
BOTH	27.36	34.04	9.55 [†]	84.66	94.36	75.55[†]

Table 2: Averaged scores for experiments of fine-tuning. F.T. means fine-tuning without any trick. * is added to zero. to show it is not a real zero-shot scenario for M2M. The bold number and the number with † follow the definition in Table 1.

methods obtain up to 0.15/0.72/0.22 for BLEU scores and 0.04/0.10/0.11 for BERTScore in en→x, x→en and zero-shot translations, respectively; For M2M-1.2B, the gain is up to 0.66/-0.38/0.21 for BLEU scores and 0.21/-0.02/0.12 for BERTScore; For mBART50, the gain is up to 0.19/0.08/4.11 for BLEU scores and 0.02/0.02/1.69 for BERTScore. Those scores show that the improvement on M2M is marginal compared with training from scratch. This derives M2M is trained by interconnected translation pairs instead of an English-centric dataset, which results in the robust transferability of multilingual representations. However, the degeneration on F.T. of mBART50 shows that fine-tuning drastically influences the zero-shot translation capacity. For instance, the BLUE scores of fr→vi decrease to 11.84 from 20.57 and fr→zh increase to 13.52 from 1.90, but our model obtains 18.47 and 17.19, respectively. Such results and the

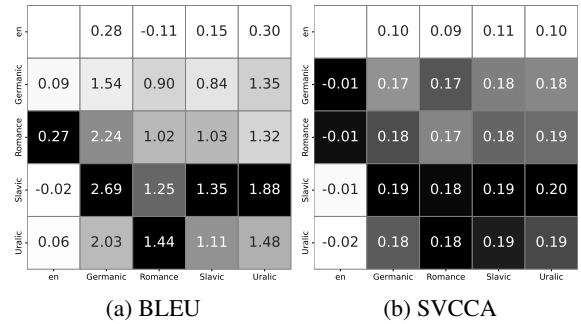


Figure 7: Differences between our model and VANILLA. X-axis is the target language family where en is considered solely. Hence, we plot the color ladder by column where the darker the color, the bigger the difference.

significant testing indicate again the advantage of our proposed methods in improving multilingual representations for zero-shot translation capacity.

6 Discussion

6.1 Correlation between Representational Disentanglements and Improvements

Table 1 shows the overall results by taking averages across all language pairs, which may overlook pair-specific tendencies. Therefore, we group Europarl-15 by the language families and report the average scores of translating from one language family to another. Figure 7a shows the difference in BLEU scores between our models and VANILLA. As shown in Figure 7b, we also compute the SVCCA scores between the identity of the non-central language and the identity of the central language at the encoder’s output and group them in the same manner. Given the similar distribution in Figure 7, we conduct Pearson correlation analysis (Pearson, 1896) of all language pairs instead of language families in Europarl-15, and we compute the coefficients and p -values of Pearson correlation by target

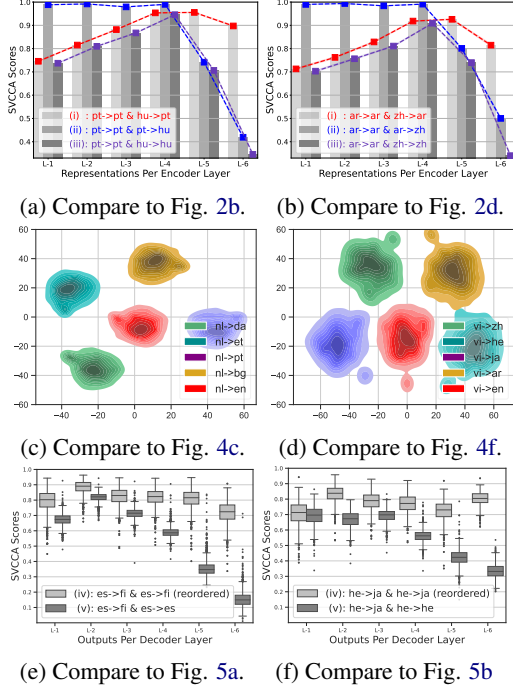


Figure 8: Visualizations for the encoder that incorporates LOLE and LCLR, showing improvements compared with VANILLA. Additionally, the model plotted in 8e only incorporates LCLR.

languages to maintain fairness. We observe two key points: 1) The coefficient and p -value of en are -0.087 and 0.76, respectively. This result suggests that there is no statistical correlation, which is predictable because $x \rightarrow en$ is not affected by representational entanglements. 2) The coefficient and p -value of non-central languages are in the ranges of 0.585 to 0.855 and $4e-5$ to 0.021, respectively. In more detail, the mean values are 0.770 and 0.002 and the variances are 0.04 and $3e-5$, respectively. This analysis proves that the degree of representational disentanglement positively correlates with the improvement of zero-shot translations.

6.2 Analysis of Improved Representation

To further verify our hypothesis, we measure representation transfer in the model incorporating our proposed methods. As shown in Figures 8a and 8b, both scenarios exhibit improvements on (i). Meanwhile, Figures 8c and 8d indicate that the entanglement of representations among languages at the encoder is resolved. The evidence suggests that LOLE effectively enhances representation transfer in the encoder. Additionally, (ii) and (iii) in Figures 8a and 8b also achieve higher scores at lower layers of the encoder, which suggests that LOLE indeed makes lower layers of the encoder focus on surface-level information. By contrast, as shown in Figures 8e and 8f, the more stable trend of (iv) in both

scenarios suggests that LCLR can improve the capacity of lower layers of the decoder to distinguish languages to improve zero-shot translations. In addition, Appendix G provides the representational analysis for fine-tuning models, which proves that target language features are consistently beneficial in the encoder.

7 Related Works

Although representational analysis can guide improving the zero-shot translation capacity in MNMT, prior analyses have shown seemingly contradictory conclusions. Kudugunta et al. (2019) found that the encoder clusters representations of different translations based on target language features, suggesting that the encoder is language-specific. However, this conclusion is indirect because comparing real translation pairs would accumulate errors, even though Gu et al. (2019); Liu et al. (2021); Qu and Watanabe (2022) can support the validity. Our work extends this conclusion by using identity pairs to show that representations of source languages are transferred to the target subspace. Notably, Zhang et al. (2021); Pires et al. (2023) reached similar conclusions by incorporating learnable weights in additional language-specific modules. Another viewpoint is that an ideal encoder is considered to learn only language-agnostic representations (Pham et al., 2019; Zhu et al., 2020; Pan et al., 2021; Gu and Feng, 2022; Gao et al., 2023). Our representational analysis demonstrates that the general cross-lingual state does not exist in the encoder and the alignment occurs within the representational subspace of the target language. Additionally, our analysis supports that delimiting the language-specific representation boundaries at the decoder side is also important (Yang et al., 2021; Chen et al., 2023).

8 Conclusion

We systematically investigated the representational issue of zero-shot translation deficiency in multilingual neural machine translation models. Our analyses show that the encoder transfers translation representations from the source language to the target language, and aligns different languages at the target language subspace. We applied engineering practices to verify our findings by proposing two orthogonal methods, which substantially improve the zero-shot translation capacity. Thus, our findings are significant for guiding the improvement of the transferability of multilingual representations.

9 Limitations

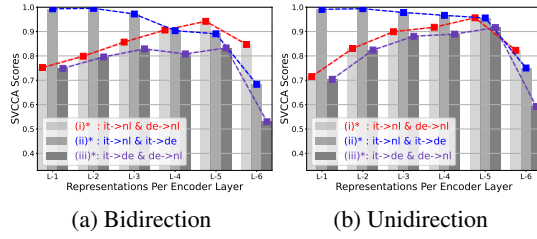


Figure 9: Illustration of the comparison between the bidirectional representation and the unidirectional representation. 9a has the same model settings with Figure 2, but the identity pairs are not employed.

This work has two limitations. First, the identity pair is a proxy of language-specific representations, which are based on bi-directional training, i.e., each non-central language appears in the encoder and decoder together. Therefore, we designed an additional study to investigate the impact by retraining a model by eliminating $n1 \rightarrow en$ and $en \rightarrow it$ so that it and $n1$ appear only in the encoder and decoder, respectively based on the analysis in Section 3.2. Then, we conducted a comparison by taking de as the middle language to perform the role of identity pairs in analysis. As shown in Figure 9, the target language features keep the same trend as shown in Section 3.2 to support our conclusion again, but the influence of source language features increases relatively.

The second limitation is our investigation is based on adding a language tag specified to the target language at the beginning of the source sentence for the encoder. Although this is the de facto MNMT training strategy (Johnson et al., 2017; Aharoni et al., 2019; Arivazhagan et al., 2019a; Gu et al., 2019; Pham et al., 2019; Wu et al., 2021; Yang et al., 2021; Pan et al., 2021; Qu and Watanabe, 2022; Chen et al., 2023; Gu and Feng, 2022; Gao et al., 2023), the current pre-trained models (Fan et al., 2020; Liu et al., 2020; Team et al., 2022) are not based on the strategy. Our methodologies are also effective in mBART50 (Liu et al., 2020) and M2M (Fan et al., 2020) because they are based on adding a source language tag for the encoder, where we can measure the effectiveness of improving the target language information. However, NLLB (Team et al., 2022) is based on two target language tags at the encoder and the decoder, respectively, whose representation transfer is not clear from the conclusions of this work. Thus, our future work is to investigate the representation transfer of NLLB.

References

- Roe Aharoni, Melvin Johnson, and Orhan Firat. 2019. [Massively multilingual neural machine translation](#). *Preprint*, arXiv:1903.00089.
- Naveen Arivazhagan, Ankur Bapna, Orhan Firat, Roe Aharoni, Melvin Johnson, and Wolfgang Macherey. 2019a. [The missing ingredient in zero-shot neural machine translation](#). *Preprint*, arXiv:1903.07091.
- Naveen Arivazhagan, Ankur Bapna, Orhan Firat, Dmitry Lepikhin, Melvin Johnson, Maxim Krikun, Mia Xu Chen, Yuan Cao, George Foster, Colin Cherry, Wolfgang Macherey, Zhifeng Chen, and Yonghui Wu. 2019b. [Massively multilingual neural machine translation in the wild: Findings and challenges](#). *Preprint*, arXiv:1907.05019.
- Liang Chen, Shuming Ma, Dongdong Zhang, Furu Wei, and Baobao Chang. 2023. [On the off-target problem of zero-shot multilingual neural machine translation](#). In *Findings of the Association for Computational Linguistics: ACL 2023*, pages 9542–9558, Toronto, Canada. Association for Computational Linguistics.
- Raj Dabre and Sadao Kurohashi. 2019. [Mmc4nlp: Multilingual multiway corpora repository for natural language processing](#). *Preprint*, arXiv:1710.01025.
- Hiroyuki Deguchi, Taro Watanabe, Yusuke Matsui, Masao Utiyama, Hideki Tanaka, and Eiichiro Sumita. 2023. [Subset retrieval nearest neighbor machine translation](#). In *Proceedings of the 61st Annual Meeting of the Association for Computational Linguistics (Volume 1: Long Papers)*, pages 174–189, Toronto, Canada. Association for Computational Linguistics.
- Angela Fan, Shruti Bhosale, Holger Schwenk, Zhiyi Ma, Ahmed El-Kishky, Siddharth Goyal, Man-deep Baines, Onur Celebi, Guillaume Wenzek, Vishrav Chaudhary, Naman Goyal, Tom Birch, Vitaliy Liptchinsky, Sergey Edunov, Edouard Grave, Michael Auli, and Armand Joulin. 2020. [Beyond english-centric multilingual machine translation](#). *Preprint*, arXiv:2010.11125.
- Orhan Firat, Baskaran Sankaran, Yaser Al-onaizan, Fatos T. Yarman Vural, and Kyunghyun Cho. 2016. [Zero-resource translation with multi-lingual neural machine translation](#). In *Proceedings of the 2016 Conference on Empirical Methods in Natural Language Processing*, pages 268–277, Austin, Texas. Association for Computational Linguistics.
- Pengzhi Gao, Liwen Zhang, Zhongjun He, Hua Wu, and Haifeng Wang. 2023. [Improving zero-shot multilingual neural machine translation by leveraging cross-lingual consistency regularization](#). In *Findings of the Association for Computational Linguistics: ACL 2023*, pages 12103–12119, Toronto, Canada. Association for Computational Linguistics.
- Jiatao Gu, Yong Wang, Kyunghyun Cho, and Victor O.K. Li. 2019. [Improved zero-shot neural machine translation via ignoring spurious correlations](#).

- In *Proceedings of the 57th Annual Meeting of the Association for Computational Linguistics*, pages 1258–1268, Florence, Italy. Association for Computational Linguistics.
- Shuhao Gu and Yang Feng. 2022. [Improving zero-shot multilingual translation with universal representations and cross-mapping](#). In *Findings of the Association for Computational Linguistics: EMNLP 2022*, pages 6492–6504, Abu Dhabi, United Arab Emirates. Association for Computational Linguistics.
- David R. Hardoon, Sandor Szedmak, and John Shawe-Taylor. 2004. [Canonical correlation analysis: An overview with application to learning methods](#). *Neural Computation*, 16(12):2639–2664.
- Edward J. Hu, Yelong Shen, Phillip Wallis, Zeyuan Allen-Zhu, Yuanzhi Li, Shean Wang, Lu Wang, and Weizhu Chen. 2021. [Lora: Low-rank adaptation of large language models](#). *Preprint*, arXiv:2106.09685.
- Li Jing, Pascal Vincent, Yann LeCun, and Yuandong Tian. 2022. [Understanding dimensional collapse in contrastive self-supervised learning](#). *Preprint*, arXiv:2110.09348.
- Melvin Johnson, Mike Schuster, Quoc V. Le, Maxim Krikun, Yonghui Wu, Zhifeng Chen, Nikhil Thorat, Fernanda Viégas, Martin Wattenberg, Greg Corrado, Macduff Hughes, and Jeffrey Dean. 2017. [Google’s multilingual neural machine translation system: Enabling zero-shot translation](#). *Transactions of the Association for Computational Linguistics*, 5:339–351.
- Urvashi Khandelwal, Angela Fan, Dan Jurafsky, Luke Zettlemoyer, and Mike Lewis. 2021. [Nearest neighbor machine translation](#). In *International Conference on Learning Representations*.
- Diederik P. Kingma and Jimmy Ba. 2017. [Adam: A method for stochastic optimization](#). *Preprint*, arXiv:1412.6980.
- Philipp Koehn. 2004. [Statistical significance tests for machine translation evaluation](#). In *Proceedings of the 2004 Conference on Empirical Methods in Natural Language Processing*, pages 388–395, Barcelona, Spain. Association for Computational Linguistics.
- Philipp Koehn et al. 2005. Europarl: A parallel corpus for statistical machine translation. In *MT summit*, volume 5, pages 79–86. Citeseer.
- Taku Kudo and John Richardson. 2018. [SentencePiece: A simple and language independent subword tokenizer and detokenizer for neural text processing](#). In *Proceedings of the 2018 Conference on Empirical Methods in Natural Language Processing: System Demonstrations*, pages 66–71, Brussels, Belgium. Association for Computational Linguistics.
- Sneha Kudugunta, Ankur Bapna, Isaac Caswell, and Orhan Firat. 2019. [Investigating multilingual NMT representations at scale](#). In *Proceedings of the 2019 Conference on Empirical Methods in Natural Language Processing and the 9th International Joint Conference on Natural Language Processing (EMNLP-IJCNLP)*, pages 1565–1575, Hong Kong, China. Association for Computational Linguistics.
- Mike Lewis, Yinhan Liu, Naman Goyal, Marjan Ghazvininejad, Abdelrahman Mohamed, Omer Levy, Ves Stoyanov, and Luke Zettlemoyer. 2019. [Bart: Denoising sequence-to-sequence pre-training for natural language generation, translation, and comprehension](#). *Preprint*, arXiv:1910.13461.
- Danni Liu, Jan Niehues, James Cross, Francisco Guzmán, and Xian Li. 2021. [Improving zero-shot translation by disentangling positional information](#). In *Proceedings of the 59th Annual Meeting of the Association for Computational Linguistics and the 11th International Joint Conference on Natural Language Processing (Volume 1: Long Papers)*, pages 1259–1273, Online. Association for Computational Linguistics.
- Yinhan Liu, Jiatao Gu, Naman Goyal, Xian Li, Sergey Edunov, Marjan Ghazvininejad, Mike Lewis, and Luke Zettlemoyer. 2020. [Multilingual denoising pre-training for neural machine translation](#). *Preprint*, arXiv:2001.08210.
- Myle Ott, Sergey Edunov, Alexei Baevski, Angela Fan, Sam Gross, Nathan Ng, David Grangier, and Michael Auli. 2019. [fairseq: A fast, extensible toolkit for sequence modeling](#). In *Proceedings of the 2019 Conference of the North American Chapter of the Association for Computational Linguistics (Demonstrations)*, pages 48–53, Minneapolis, Minnesota. Association for Computational Linguistics.
- Xiao Pan, Mingxuan Wang, Liwei Wu, and Lei Li. 2021. [Contrastive learning for many-to-many multilingual neural machine translation](#). In *Proceedings of the 59th Annual Meeting of the Association for Computational Linguistics and the 11th International Joint Conference on Natural Language Processing (Volume 1: Long Papers)*, pages 244–258, Online. Association for Computational Linguistics.
- Kishore Papineni, Salim Roukos, Todd Ward, and Wei-Jing Zhu. 2002. [Bleu: a method for automatic evaluation of machine translation](#). In *Proceedings of the 40th Annual Meeting of the Association for Computational Linguistics*, pages 311–318, Philadelphia, Pennsylvania, USA. Association for Computational Linguistics.
- Karl Pearson. 1896. [Mathematical contributions to the theory of evolution. iii. regression, heredity, and panmixia](#). *Philosophical Transactions of the Royal Society of London. Series A, Containing Papers of a Mathematical or Physical Character*, 187:253–318.
- Ngoc-Quan Pham, Jan Niehues, Thanh-Le Ha, and Alexander Waibel. 2019. [Improving zero-shot translation with language-independent constraints](#). In *Proceedings of the Fourth Conference on Machine Translation (Volume 1: Research Papers)*, pages 13–23,

- Florence, Italy. Association for Computational Linguistics.
- Telmo Pires, Robin Schmidt, Yi-Hsiu Liao, and Stephan Peitz. 2023. [Learning language-specific layers for multilingual machine translation](#). In *Proceedings of the 61st Annual Meeting of the Association for Computational Linguistics (Volume 1: Long Papers)*, pages 14767–14783, Toronto, Canada. Association for Computational Linguistics.
- Matt Post. 2018. [A call for clarity in reporting BLEU scores](#). In *Proceedings of the Third Conference on Machine Translation: Research Papers*, pages 186–191, Brussels, Belgium. Association for Computational Linguistics.
- Zhi Qu and Taro Watanabe. 2022. [Adapting to non-centered languages for zero-shot multilingual translation](#). In *Proceedings of the 29th International Conference on Computational Linguistics*, pages 5251–5265, Gyeongju, Republic of Korea. International Committee on Computational Linguistics.
- Maithra Raghu, Justin Gilmer, Jason Yosinski, and Jascha Sohl-Dickstein. 2017. Svcca: Singular vector canonical correlation analysis for deep learning dynamics and interpretability. In *Proceedings of the 31st International Conference on Neural Information Processing Systems, NIPS’17*, page 6078–6087, Red Hook, NY, USA. Curran Associates Inc.
- Naomi Saphra and Adam Lopez. 2019. [Understanding learning dynamics of language models with SVCCA](#). In *Proceedings of the 2019 Conference of the North American Chapter of the Association for Computational Linguistics: Human Language Technologies, Volume 1 (Long and Short Papers)*, pages 3257–3267, Minneapolis, Minnesota. Association for Computational Linguistics.
- Sukanta Sen, Kamal Kumar Gupta, Asif Ekbal, and Pushpak Bhattacharyya. 2019. [Multilingual unsupervised NMT using shared encoder and language-specific decoders](#). In *Proceedings of the 57th Annual Meeting of the Association for Computational Linguistics*, pages 3083–3089, Florence, Italy. Association for Computational Linguistics.
- NLLB Team, Marta R. Costa-jussà, James Cross, Onur Çelebi, Maha Elbayad, Kenneth Heafield, Kevin Heffernan, Elahe Kalbassi, Janice Lam, Daniel Licht, Jean Maillard, Anna Sun, Skyler Wang, Guillaume Wenzek, Al Youngblood, Bapi Akula, Loic Barrault, Gabriel Mejia Gonzalez, Prangthip Hansanti, John Hoffman, Semaire Jarrett, Kaushik Ram Sadagopan, Dirk Rowe, Shannon Spruit, Chau Tran, Pierre Andrews, Necip Fazil Ayan, Shruti Bhosale, Sergey Edunov, Angela Fan, Cynthia Gao, Vedanuj Goswami, Francisco Guzmán, Philipp Koehn, Alexandre Mourachko, Christophe Ropers, Safiyyah Saleem, Holger Schwenk, and Jeff Wang. 2022. [No language left behind: Scaling human-centered machine translation](#). *Preprint*, arXiv:2207.04672.
- Yuandong Tian. 2022. [Understanding deep contrastive learning via coordinate-wise optimization](#). In *Advances in Neural Information Processing Systems*.
- Laurens van der Maaten and Geoffrey Hinton. 2008. [Visualizing data using t-sne](#). *Journal of Machine Learning Research*, 9(86):2579–2605.
- Ashish Vaswani, Noam Shazeer, Niki Parmar, Jakob Uszkoreit, Llion Jones, Aidan N Gomez, Łukasz Kaiser, and Illia Polosukhin. 2017. [Attention is all you need](#). In *Advances in Neural Information Processing Systems*, volume 30. Curran Associates, Inc.
- M. P. Wand and M. C. Jones. 1993. [Comparison of smoothing parameterizations in bivariate kernel density estimation](#). *Journal of the American Statistical Association*, 88(422):520–528.
- Liwei Wu, Shanbo Cheng, Mingxuan Wang, and Lei Li. 2021. [Language tags matter for zero-shot neural machine translation](#). In *Findings of the Association for Computational Linguistics: ACL-IJCNLP 2021*, pages 3001–3007, Online. Association for Computational Linguistics.
- Frank F. Xu, Uri Alon, and Graham Neubig. 2023. [Why do nearest neighbor language models work?](#) *Preprint*, arXiv:2301.02828.
- Yilin Yang, Akiko Eriguchi, Alexandre Muzio, Prasad Tadepalli, Stefan Lee, and Hany Hassan. 2021. [Improving multilingual translation by representation and gradient regularization](#). In *Proceedings of the 2021 Conference on Empirical Methods in Natural Language Processing*, pages 7266–7279, Online and Punta Cana, Dominican Republic. Association for Computational Linguistics.
- Qi Ye, Sachan Devendra, Felix Matthieu, Padmanabhan Sarguna, and Neubig Graham. 2018. When and why are pre-trained word embeddings useful for neural machine translation. In *HLT-NAACL*.
- Biao Zhang, Ankur Bapna, Rico Sennrich, and Orhan Firat. 2021. [Share or not? learning to schedule language-specific capacity for multilingual translation](#). In *International Conference on Learning Representations*.
- Biao Zhang, Philip Williams, Ivan Titov, and Rico Sennrich. 2020a. [Improving massively multilingual neural machine translation and zero-shot translation](#). In *Proceedings of the 58th Annual Meeting of the Association for Computational Linguistics*, pages 1628–1639, Online. Association for Computational Linguistics.
- Tianyi Zhang, Varsha Kishore, Felix Wu, Kilian Q. Weinberger, and Yoav Artzi. 2020b. [Bertscore: Evaluating text generation with bert](#). *Preprint*, arXiv:1904.09675.
- Changfeng Zhu, Heng Yu, Shanbo Cheng, and Weihua Luo. 2020. [Language-aware interlingua for multilingual neural machine translation](#). In *Proceedings*

A Sentence-level SVCCA Score

We use SVCCA (Raghu et al., 2017) to measure representation similarity in MNMT (Kudugunta et al., 2019). We follow the approach of Liu et al. (2021) so that similarity is measured at the sentence level to ensure that each score is computed on equivalent features without the influence of other sentences in the set.

Based on the definition of Section 2.1, we denote hidden representations of a sentence by $\mathbf{H} = \{\mathbf{h}_1, \mathbf{h}_2, \dots, \mathbf{h}_q\}$, where $\mathbf{H} \in \mathbb{R}^{q \times d}$, q equals to the length n or m from either the encoder or decoder, and d is the model dimension. Additionally, the practical length is $n + 1$ when \mathbf{H} is fed into the encoder because the encoder receives the input concatenated by l and \mathbf{x} . Then, we derive the sentence-level representation $\bar{\mathbf{h}}$ using average pooling $\bar{\mathbf{h}} = \frac{\sum_{i=1}^q \mathbf{h}_i}{q}$, which mainly represents the language features and semantics of the source sentence rather than syntactic information because positional information is reduced.

Given \mathbf{H}^a and \mathbf{H}^b derived from two sentences, SVCCA first performs singular value decomposition on their averaged representations to obtain subspace representations $\bar{\mathbf{h}}^a \in \mathbb{R}^{d^a}$ and $\bar{\mathbf{h}}^b \in \mathbb{R}^{d^b}$, where noise is reduced (Saphra and Lopez, 2019). Then we perform canonical correlation analysis (Hardoon et al., 2004) to determine $\mathbf{W}^a \in \mathbb{R}^{d' \times d^a}$ and $\mathbf{W}^b \in \mathbb{R}^{d' \times d^b}$. Formally, we compute correlation ρ between $\bar{\mathbf{h}}^a$ and $\bar{\mathbf{h}}^b$ as

$$\rho = \frac{\langle \mathbf{W}^a \bar{\mathbf{h}}^a, \mathbf{W}^b \bar{\mathbf{h}}^b \rangle}{\|\mathbf{W}^a \bar{\mathbf{h}}^a\| \|\mathbf{W}^b \bar{\mathbf{h}}^b\|}, \quad (5)$$

where $\langle \cdot, \cdot \rangle$ indicates the inner product. We use ρ to represent the similarity of two sentences. Finally, we compute the set-level score by taking the average scores of all sentences over the set.

B Detailed Information of Datasets

This work involves three datasets, i.e., Europarl-15, TED-19, and OPUS-100, where Europarl-15 and TED-19 are used in preliminary experiments.

Europarl-15 is collected from MMCR4NLP, which has high-quality sentences and each sentence in a language is one-to-one corresponding to other languages, i.e., all language-specific sets

have parallel semantics (Koehn et al., 2005; Dabre and Kurohashi, 2019), including 15 European languages from 4 language families. Specifically, Germanic includes en, de, nl, da, Romance includes es, pt, it, ro, Slavic includes sl, bg, pl, cs, and Uralic includes fi, et, hu. The training and validation sets cover 28 supervised language pairs where English is the central language used to bridge the non-central languages. The test set consists of all language pairs, including 182 zero-shot language pairs in addition to supervised language pairs. Each pair in the training set comprises 189,310 sentences. The validation and test sets for each pair contain 2,000 sentences, and we measure SVCCA scores in the test sets.

In contrast to the aligned corpus, TED-19 consists of 19 languages, including en, ar, he, ru, ko, it, ja, zh, es, nl, vi, tr, fr, pl, ro, fa, hr, cs, de, which belong to various language families without parallel semantics, from TED Talks (Ye et al., 2018). Each pair contains 103,093 to 214,111 sentences in training. The training set comprises 6,551,456 sentences in total, and the validation and test sets for each pair contain 2,000 sentences. Because of the unparallel semantics of TED-19, we align ar, he, zh, hr, vi, ja to obtain 967 sentences for measuring SVCCA scores. In addition, the reason why the number of languages is 19 is that, first, TED Talks have 20 high-resource languages, which are supported in M2M (Fan et al., 2020) and mBART50 (Liu et al., 2020). However, the tokenization of th is problematic, resulting in deprecating th.

OPUS-100 consists of 95 languages, 188 pairs, and 109.2 million samples in total (Zhang et al., 2020a; Yang et al., 2021), where 90 pairs comprise 1 million samples and 56 pairs have more than 0.1 million samples. Different from Yang et al. (2021), we do not use the provided valid set for zero-shot translation pairs in training to avoid biases when assessing the transferability of multilingual representations.

C Detailed Settings of Models

We use the Transformer (Vaswani et al., 2017) from Fairseq (Ott et al., 2019) as the model. For the configuration of models trained on Europarl-15 and TED-19, we follow Kudugunta et al. (2019) to set 6 encoder and decoder layers. In addition, we investigate models in Appendix E with 8 and 10 encoder layers. We adopt a shared vocabulary trained by

SentencePiece (Kudo and Richardson, 2018) with 50,000 tokens for both the encoder and decoder. The model consists of 4 attention heads, embedding size of 512, inner size of 1024, dropout rate of 0.2, maximum learning rate of 0.0005 with the inverse square root schedule and 4,000 warmup steps, and label smoothing rate of 0.1. We set the batch size to 8,000 tokens per GPU, apply Adam (Kingma and Ba, 2017) as the optimizer, and set temperature sampling with $T = 5$ (Arivazhagan et al., 2019b). We train the model with 60 epochs for Europarl-15 and 30 epochs for TED-15, and finally average the top 5 checkpoints using the loss on the validation set. Compared with the basic configuration, the models trained on OPUS-100 have 8 attention heads, embedding size of 512, inner size of 2048, dropout rate of 0.1, and shared vocabulary size of 64,000. We train the model of OPUS-100 for 400,000 update steps with a batch size of 8,000 tokens per GPU for OPUS-100 and directly use the best checkpoint selected using the loss on the validation set. Furthermore, models with Europarl-15 and TED-19 are trained on 8 NVIDIA V100 GPUs, and models with OPUS-100 are trained on 4 NVIDIA A6000 GPUs by setting `-update-freq` to 2 in Fairseq to simulate 8 GPUs.

Three pre-trained models are utilized in our experiments. The first is M2M-418M (Fan et al., 2020), a model trained on standard multilingual translation tasks, that supports translation across 100 languages. It is based on Transformer architecture, configured with 12 encoder and decoder layers, embedding size of 1024, inner size of 4096, and vocabulary size of 128,112, which results in a total of 418 million parameters. The second model, M2M-1.2B (Fan et al., 2020), extends the M2M-418M by enlarging the number of layers to 24 and the inner size to 8192, which culminates in 1.2 billion parameters. The last model is mBART50 (Liu et al., 2020), which was trained on monolingual corpora across 50 languages following Lewis et al. (2019) and preliminarily fine-tuned for multilingual translation tasks. It shares the same parameter setup as M2M-418M with a vocabulary size of 250,053, which consists of 611 million parameters. We conduct experiments on TED-19 because all covered languages are supported by these models.

D Detailed Introductions of Figure 1

In fact, Figure 1a corresponds to the last subfigure of Figure 10 to show the linguistic affin-

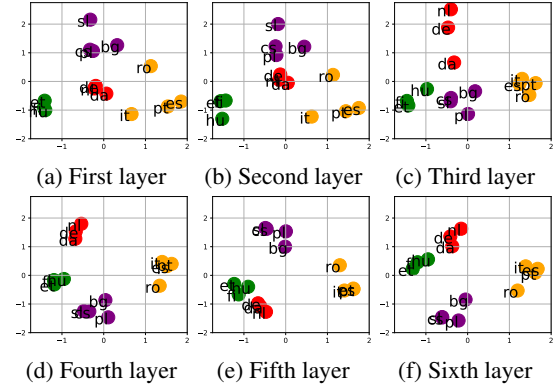


Figure 10: Affinities for $en \rightarrow x$ at each encoder layer. Language families of Europarl-15 are distinguished by colors: Germanic by red, Romance by yellow, Slavic by purple, and Uralic by green.

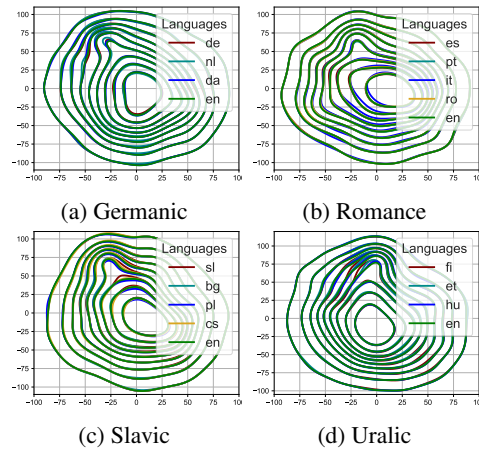


Figure 11: Visualizations by t-SNE and BiKDE of aligning representations between $en \rightarrow en$ and $x \rightarrow en$ of Europarl-15 at the output of the encoder.

ity between translations from English to other languages, denoted by $en \rightarrow x$. Specifically, Figure 10 shows the layer-wise states of the encoder, and Figure 1a (Figure 10f) demonstrates the state at the output of the encoder. We employ *sklearn.manifold.SpectralEmbedding*, referring to <https://scikit-learn.org>, to visualize the similarities computed by SVCCA (Appendix A) for every layer in the encoder. Then, we can find that representations at all encoder layers have certain clusters influenced by the families of the target languages, and the clusters become more distinct as the depth of the encoder layers increases. This suggests that the transfer of representations to the target language begins as early as the first layer of the encoder, with gradual strengthening through further layers. Meanwhile, this finding, i.e., even the initial encoder layers capture target language features, complements prior works (Kudugunta et al., 2019; Pires et al., 2023).

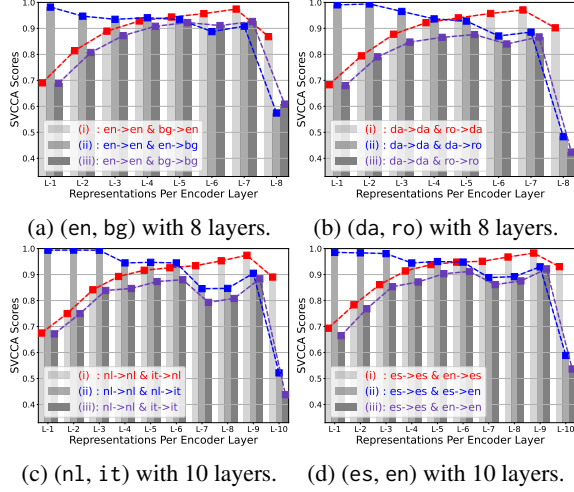


Figure 12: Visualizations of 8 and 10 encoder layers on Europarl-15 languages, which are different from Figure 2 as a comparison to prove the generalization.

On the other hand, we follow Pan et al. (2021) and Gao et al. (2023) to measure the alignment of encoder representations between the identity of en and source languages from different families to English using t-distributed stochastic neighbor embedding (t-SNE) (van der Maaten and Hinton, 2008) and bivariate kernel density estimation (BiKDE) (Wand and Jones, 1993). As shown in Figure 11, representations from the four language families are all highly aligned with the identity pair of en \rightarrow en, where the common feature of those translations is the parallel semantics. Thus, this proves that the encoder semantically aligns different translations. However, the deep discussion should be referred to Section 3.2.

E Investigation on Models with 8 and 10 Encoder Layers

Figure 12 shows the scenarios of 8 and 10 encoder layers to confirm our conclusion, where all the cases for (i) consistently reflect the same tendency. Together with the increased number of layers, the increased final scores of (i) indicate the stronger target language features of ① presented for representations. Meanwhile, we also observe that the scores of (iii) are close to or even exceed those of (ii) at some layers both in Figures 2 and 12. This proves that the feature of the source language is not the primary factor for representations in the encoder because representations are transferred to the subspaces of target languages. Thus, this further investigation supports our conclusion that language transferred within the encoder is general.

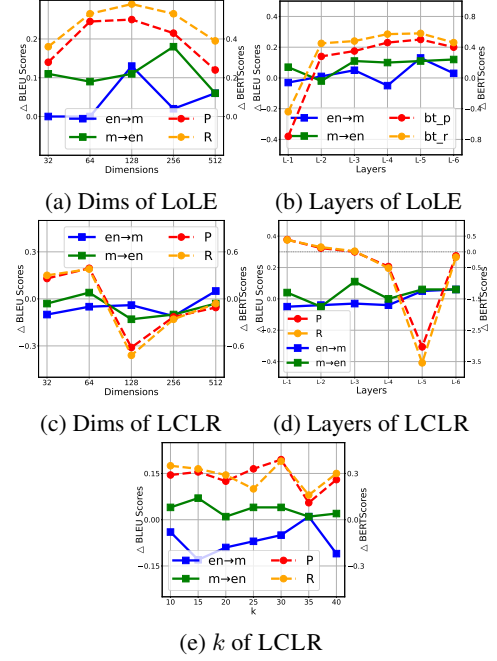


Figure 13: Illustrations for the ablation study. Δ means the difference between the scores of our methods and the scores of VANILLA. 13a and 13b present variations of LoLE in dimensions and layers, respectively; and 13c, 13d, and 13e present variations of LCLR in dimensions, layers, and k , respectively.

F Selecting Hyper-Parameters

We conduct ablation studies on the validation set of Europarl-15 to select hyper-parameters for LoLE and LCLR, which are used in Section 5.1. Figure 13a shows that LoLE performs optimally with the dimension of 128, which corroborates our hypothesis in Section 4.1. Figure 13b indicates that LoLE performs the best at the fifth layer and degrades significantly at lower layers, which aligns with our assertion in Section 3.2 that lower layers of the encoder are more correlated with the source language, and enhances the language transfer benefits of transferability (Section 4.1). Figure 13c is consistent with the theory of contrastive learning in which full dimensions lead to collapse (Jing et al., 2022). Figure 13d demonstrates that, as the position constructed by LCLR increases, the scores decrease, which lends support to our analysis in Sections 3.4 that the instability of decoder representations primarily manifests at lower layers, which also explains the weakness of TLP because improving the capacity of distinguishing languages is redundant for the decoder’s top layer. We also conduct an ablation study for hyperparameter k for LCLR with a dimension of 64 at the bottom decoder layer. The results are shown in Figure 13e,

	Pairs	Model	Method	(i)	(ii)	(iii)
Encoder Side	① of zh ② of ar	M2M	F.T.	79.66	100.0	79.66
			LoLE	79.52	98.75	77.76
		mBART	F.T.	63.97	100.0	63.97
			LoLE	63.52	97.90	61.66
	① of he ② of vi	M2M	F.T.	81.50	100.0	81.50
			LoLE	80.54	98.27	79.88
Decoder Side		mBART	F.T.	69.17	100.0	69.17
			LoLE	70.46	97.61	67.04
	① of ja ② of he	M2M	F.T.	99.80	92.01	92.65
			LoLE	99.73	89.81	90.66
		mBART	F.T.	98.53	90.76	89.62
			LoLE	98.64	90.07	88.49

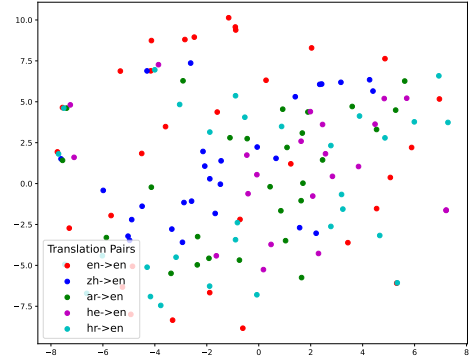
Table 3: SVCCA scores. Each score times 100 for a clear illustration. (i) compares the identity of ① and ①→②, (ii) compares the identity of ① and ②→①, and (iii) compares identities of ① and ②. Encoder Side means computing the output of the encoder, and Decoder Side means computing the output of the 1st layer of the decoder.

with an empirically optimal $k = 30$.

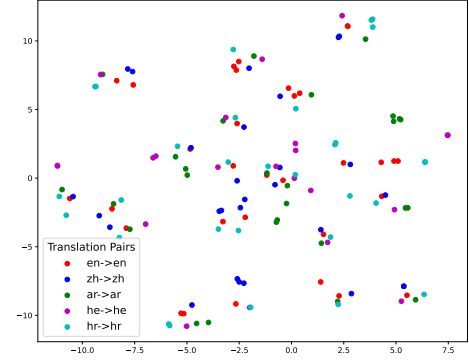
G Analysis of Improved Representation for Fine-tuning Pre-trained Models

Section 6.2 is the representational analysis for models, which are trained from scratch with proposed LOLE and LCLR. We also show the representational analysis for fine-tuning pre-trained models.

Given the positive correlation shown in Section 6.1, we compute SVCCA scores in the same way as done in Section 3.2 and show the results in Table 3. Unlike Section 3.2, we equally consider the encoder and decoder because the encoder is only related to the source language and does not transfer representations to the target language in the training strategy of M2M (Fan et al., 2020) and mBART50 (Liu et al., 2020). Additionally, the different training strategy is the primary reason that F.T. shows the same scores in (i) and (iii) and keeps 100.0 in (ii). Alternatively, although the scores of (i), which reflect target language features, decrease in our methods, the scores of (ii) and (iii) also decrease. As a result, the differences between the scores of (i), (ii), and (iii) increase, that is, the relative importance of target language features increases. This result proves our statements in Sections 3.3 and 6.1 again that target language features are consistently beneficial in the encoder. On the other hand, the decoder side shows the same tendency as the encoder side. This fits our motivation in Section 4.2 to further improve the discriminating ability of lower layers of the decoder, although the training strategy of M2M and mBART50 has already



(a) Semantic alignments on embeddings



(b) Semantic alignments on identities

Figure 14: Illustration of the token-level alignment corresponding to Figure 1b. Representations shown in 14a are collected at the embedding layer, whose overall variance is 1.45. Representations shown in 14b are collected from identities, whose overall variance is 0.13.

provided a high capacity in discrimination for the decoder.

H Token-level Alignments in Other Cases

First of all, the English sentence for semantic analysis in Figures 3 and 14 is: By the end of this year, there will be nearly a billion people on this planet that actively use social networking sites. Compared with the discussion in Section 3.2, token-level representations are not aligned at the embedding layer, and are relatively aligned in the case of using the identity pairs, where the degree of divergence is substantially higher than the case of Figure 3.